Author/s:
Peterson, TJ;Western, AW;Argent, RM

Title:
Multiple hydrological attractors under stochastic daily forcing: 2. Can multiple attractors emerge?

Date:
2014-04-01

Citation:
Peterson, T. J., Western, A. W. & Argent, R. M. (2014). Multiple hydrological attractors under stochastic daily forcing: 2. Can multiple attractors emerge?. WATER RESOURCES RESEARCH, 50 (4), pp.3010-3029. https://doi.org/10.1002/2012WR013004.

Persistent Link:
https://hdl.handle.net/11343/297401

AGU PUBLICATIONS

Water Resources Research

RESEARCH ARTICLE
10.1002/2012WR013004

Companion to *Peterson and Western* [2014] doi:10.1002/2012WR013003.

Key Points:
- Stochastic daily forcing can switch a catchment to both attractors
- Emergence of attractors differs significantly from the existence of attractors
- Switching between attractor basins can be subtle and difficult to identify

Correspondence to:
T. J. Peterson,
timjp@unimelb.edu.au

Citation:
Peterson, T. J., A. W. Western, and R. M. Argent (2014), Multiple hydrological attractors under stochastic daily forcing: 2. Can multiple attractors emerge?, *Water Resour. Res.*, *50*, 3010–3029, doi:10.1002/2012WR013004.

Received 25 SEP 2012
Accepted 4 MAR 2014
Accepted article online 10 MAR 2014
Published online 14 APR 2014

Multiple hydrological attractors under stochastic daily forcing: 2. Can multiple attractors emerge?

T. J. Peterson[1], A. W. Western[1], and R. M. Argent[2]

[1]Department of Infrastructure Engineering, University of Melbourne, Melbourne, Victoria, Australia, [2]Environment and Research Division, Bureau of Meteorology, Melbourne, Victoria, Australia

Abstract The companion paper showed that multiple steady state groundwater levels can exist within a hill-slope Boussinesq-vegetation model under daily stochastic forcing. Using a numerical limit-cycle continuation algorithm, the steady states (henceforth attractors) and the threshold between them (henceforth repellor) were quantified at a range of saturated lateral conductivity values, $k_{s_{max}}$. This paper investigates if stochastic daily forcing can switch the catchment between both of the attractors. That is, an attractor may exist under average forcing conditions but can stochastic forcing switch the catchment into and out of each of the attractor basins?; i.e., making the attractor emerge. This was undertaken using the model of the companion paper and by completing daily time-integration simulations at six values of the saturated lateral hydraulic conductivity, $k_{s_{max}}$; three having two attractors and three having only a deep water table attractor. By graphically analyzing the simulations, and comparing against simulations from a model modified to have only one attractor, multiple attractors were found to emerge under stochastic daily forcing. However, the emergence of attractors was significantly more subtle and complex than that suggested by the companion paper. That is, an attractor may exist but never emerge; both attractors may exist and both may emerge but identifying the switching between attractors was often ambiguous; and only one attractor may exist and but a second temporary attractor may exist and emerge during periods of high precipitation. This subtle and complex emergence of attractors was explained using continuation analysis of the climate forcing rate, and not a model parameter such as $k_{s_{max}}$. It showed that the temporary attractor existed over a large range of $k_{s_{max}}$ values and this suggests that more catchments may have multiple attractors than suggested by the companion paper. By combining this continuation analysis with the time-integration simulations, hydrological signatures indicative of a switch of multiple attractors were proposed. These signatures may provide a means for identifying actual catchments that have switched between multiple attractors.

1. Introduction

Recently, hydrology has progressed from identifying multiple hydrological attractors and positive feedbacks within simple theoretical models to developing more physically plausible models [*Peterson et al*., 2009a; *Runyan and D'Odorico*, 2010; *Peterson and Western*, 2014] and using observation data to parameterize or assess model predictions of multiple attractors [*Rennermalm et al*., 2010; *Peterson*, 2009; *Hilt et al*., 2011; *Heffernan*, 2008; *D'Odorico et al*., 2011; *D'Odorico and Porporato*, 2004; *Carpenter and Lathrop*, 2008]. However, as discussed within the companion paper (Peterson and Western, submitted manuscript), the multiple steady states (henceforth referred to as *attractors*) have been identified using annual or monthly mean climate forcing. Compared to using higher frequency climate forcing, this can result in the incorrect identification of multiple attractors (Peterson and Western, submitted manuscript). Furthermore, knowledge of the existence of multiple attractors provides no insights as to whether the system is likely to switch between the attractors. That is, a catchment may converge to, say, a deep water table attractor but the climate variability may be sufficiently low that no plausible rainfall event is adequate to cause a switch to a shallow water table attractor; making the shallow attractor practically superfluous. There is also little understanding of what the streamflow and groundwater level dynamics would look like from a catchment switching between attractors. Finally, as recently demonstrated using a very simple 1-D groundwater model with a vegetation-related positive feedback [*Peterson et al*., 2012], the interaction between the attractors and stochastic forcing data can be complex. This paper investigates these issues using the hypothetical semidistributed hill-slope ecohydrological model of Peterson and Western (submitted manuscript) in which a positive

feedback arises when the saline water table intersects the root zone and causing a reduction in LAI and an increase in recharge and hence water level (see Peterson and Western, submitted manuscript, Figure 3 for details). Specifically, this paper investigates if a physically plausible catchment model under stochastic daily forcing can switch between multiple attractors found to exist and, if so, how this may occur. That is, can the attractors not only exist but actually emerge?

Looking more broadly at multiple attractors and the concept of ecosystem resilience, the magnitude and frequency of disturbances is integral. A disturbance is considered to be a temporary deviation from the usual and *Holling* [1973] defines resilience as the magnitude of the disturbance that a system can absorb without undergoing a regime shift. In a more recent review of various biophysical systems thought to have multiple attractors, *Scheffer et al*. [2001] states that a sufficiently severe disturbance of the ecosystem state may bring the system into the basin of attraction of another state. However, *Scheffer and Carpenter* [2003] state that the way in which dynamic systems respond to environmental fluctuations is still poorly explored and an important question is how the frequency of environmental disturbances affects the probability that the system will shift to another attractor. Typically, equilibrium continuation analysis has been used to quantify the state variable location of attractors and repellors with a change in a single model parameter. The state variable distance between an attractor and repellor is then measured and inferred as the cumulative disturbance the system can absorb without switching to an alternative basin of attraction [e.g., *May*, 1977; *Walker et al*., 1981; *Ludwig et al*., 1997; *Anderies*, 2005]. While an informative technique, continuation analysis provides no insight into the magnitude or stochastic nature of the disturbance(s) required to displace the system into a different basin of attraction. For example, continuation analysis may indicate that two attractors exist for a system but the stochastic disturbances may never be of sufficient magnitude or duration to cause a crossing of a repellor, and thus, the second attractor basin may effectively not exist.

Resilience investigations into the effect of the frequency and magnitude of disturbances has been undertaken for one-dimensional systems [*Peterson et al*., 2012; *D'Odorico et al*., 2005; *Guttal and Jayaprakash*, 2007; *Møller et al*., 2009], and more recently with the inclusion of a spatial dimension [*Dakos et al*., 2010; *Guttal and Jayaprakash*, 2009; *Serizawa et al*., 2009]. The 1-D studies investigated stochastic disturbances applied to simple nonspatial deterministic models. *Guttal and Jayaprakash* [2007] investigated two well established bistable models, namely one of nutrient cycling within a shallow lake and the other of soil water-vegetation biomass for semiarid regions, and input stochastic disturbances derived from a uniform and serially uncorrelated distribution. The disturbances for the two models were nutrient loading and rainfall, respectively, and time-integration solutions from different initial conditions were derived for a range in the mean magnitude of the disturbance. Comparison of the results with equilibrium continuation found that the range in mean disturbance having two attractors contracted under stochastic forcing, with multiple attractors disappearing when the variance of the disturbance became large. However, our examination of their time series results indicates that, for the high variance disturbances, both attractors do still exist but switching between them occurs repeatedly.

Like many resilience studies, *Guttal and Jayaprakash* [2007] assumed that disturbances cause a change of attractors by pushing the model state over the repellor. However, *Peterson et al*. [2012] has shown this to be questionable. Using a very simple 1-D groundwater model with a vegetation-related positive feedback, stochastic annual precipitation was shown to cause a switch of attractors by the temporary loss of the attractor the system was within prior to the disturbance; rather than by pushing the model state across the repellor. If the disturbance was of sufficient duration then the system switched to the only existing attractor [*Peterson et al*., 2012]. To illustrate this, Figure 1a shows a *cup-and-ball* resilience diagram [*Walker et al*., 2004; *Beisner et al*., 2003] of the 1-D groundwater model for a constant rainfall. To explain the figure, the deep and shallow water table attractor basins are each represented by a *cup*, each attractor by the bottom of each *cup* and between them a threshold, that is the repellor. The state of the aquifer at a given time is represented by a *ball*, the *x* axis represents the depth to water table and the *y* axis represents the somewhat vague resilience concept [*Guttal and Jayaprakash*, 2007; *Beisner et al*., 2003; *Scheffer and Carpenter*, 2003; *Scheffer et al*., 2001] of "*effective potential*" [*Guttal and Jayaprakash*, 2007] and can be considered as the cumulative disturbance required to produce a given displacement from an attractor; the slope of which denotes the rate of recovery of the aquifer state toward each attractor [see *Peterson et al*., 2012, for Lyapunov stability curves quantifying the *effective potential*]. The shape and position of each *cup* changes with the rainfall. For example, during wet years the deep and shallow attractors shift to a shallower water table

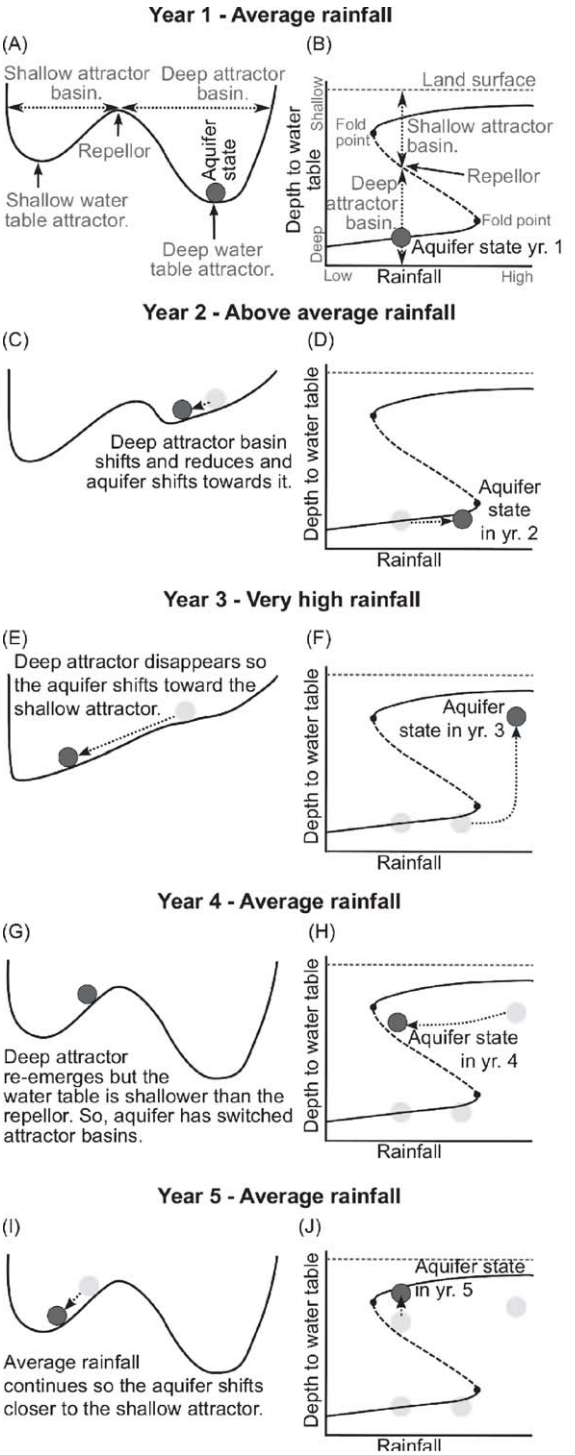

Figure 1. Schematic of how stochastic forcing causes a switching of attractor basins without crossing the repellor. (left column) Subfigures depict the change in the attractors and repellor with a change in annual rainfall. The state of the aquifer is represented by the dark gray circle and the *x* axis represents the depth to water table and the *y* axis represents the somewhat vague resilience concept of *effective potential* and can be considered as the cumulative disturbance required to produce a given displacement from an attractor; the slope of which denotes the rate of recovery of the aquifer state toward each attractor. (right column) Subfigures depict the state space location of the attractors (solid line) and the repellor (dashed line) with a change in the annual rainfall. The state of the aquifer is represented by the dark gray circle and the *y* axis represents the depth to water table and is reversed. See subfigures (a and b) for additional details.

depth, the depth of the shallow attractor increases (i.e., its *cup* size increases), the depth of the deep attractor declines (i.e., its *cup* size reduces) and the repellor moves closer to the deep attractor (see Figures 1a and 1c). The occurrence of a wet year also changes the state of the aquifer. In Figure 1a, the aquifer state is at the deep attractor but the occurrence of a wet year shifts the deep attractor (see Figure 1c) so the aquifer water level rises toward it and, if the wet period persists for a number of years, the water level would converge to the deep attractor (Figure 1c denotes this by the *ball* rolling toward the deep attractor). These dynamics are also depicted by equilibrium continuation plots within the right-hand column of Figure 1. Instead of showing the shape of the attractor basins for a fixed rainfall, the equilibrium continuations plots show how the attractors and repellor change with rainfall. The maximum rainfall at which the deep attractor exists is also denoted by the fold point; and vice versa for the shallow attractor. Additionally, the aquifer state is denoted and, like the *cup-and-ball* diagrams, the occurrence of a wet year (see Figure 1d) causes the deep attractor basin to narrow and the aquifer state shifts to below the deep attractor line because it is no longer at a steady state.

To illustrate how the aquifer changes from the deep to the shallow attractor without crossing the repellor, consider the following sequence of years. Year 1 has an average rainfall and two attractors exist (Figure 1a). For many years prior, average rainfall had occurred and the aquifer state had converged to the deep attractor. In year 2 above average rainfall occurs and, as shown in Figure 1c, both the shallow and deep attractors shift to a shallower water

level. The deep attractor basin also reduces and this is shown in Figure 1d by the aquifer state being close to the right fold-point. The aquifer state responds to the increased rainfall and, as shown in Figure 1c, the water level rises toward the deep attractor. In year 3 very high rainfall occurs and, as shown in Figure 1f, the right fold-point is exceeded. Consequently, only the shallow attractor basin exists and, as shown in Figure 1e, the shallow attractor shifts to a shallower water level. The aquifer state responds by the water level rising near to the shallow attractor. In year 4 average rainfall returns and, consequently, two attractors exist. The aquifer water level responds by declining but, during the prior year it had risen sufficiently that, upon a return to average rainfall, the water level is slightly shallower than the repellor (see Figure 1g). In year 5 average rainfall continues and, hence, the attractor basins do not change shape and the aquifer water level responds by converging closer to the shallow attractor. In summary, stochastic forcing causes a switch of attractor basins when a fold point is exceeded and the system responds sufficiently quickly that, upon return to forcing conditions at which multiple attractors exist, the system is on the alternate side of the repellor. For this example, to switch back to the deep attractor basin a similar mechanism is required whereby a period of sufficiently low rainfall shifts the system below the lower fold-point where only the deep attractor exists.

These attractor switching mechanisms can also lead to complex dynamics where only one attractor exists for average forcing conditions but under wetter conditions a second attractor exists. To illustrate, consider the scenario that under average rainfall the aquifer state in Figure 1b is now just to the left of the lower fold-point so that only the deep attractor exists. In year 2, high rainfall occurs and the aquifer state shifts to the right of the left fold-point and two attractors now exist. In year 3, the rainfall is very high and the aquifer state shifts past the right fold-point, at which time only the shallow attractor exists. Like the above scenario, the aquifer water level responses by rising near to the shallow attractor. The aquifer will persist within this temporary shallow attractor until average rainfall returns; at which time only the deep attractor exists and, if average rainfall persists, the aquifer water level will respond by converging back to the deep attractor.

Returning to the 1-D modeling of *Guttal and Jayaprakash* [2007], two types of disturbance were addressed; namely multiplicative and additive noise. Additive noise is where the impact of the noise is independent of the model state variables. For example, their phosphorus cycling lake eutrophication model experienced additive noise because the time varying nutrient loading rate was simply added to the differential equation, making the noise independent of the model state variable. Multiplicative noise is where the impact of the noise is a function of the model state and as such can result in more complex dynamics. For example, their soil-vegetation model experienced multiplicative noise because the rainfall was multiplied by the function $\frac{B}{1+\lambda B}$, where B is the state variable for vegetation biomass and λ is a parameter for vegetation water use. At a high biomass the impact of large rainfall events are amplified, but conversely at a low biomass high rainfall events produce little change in vegetation biomass. When the biomass equals zero, rainfall noise is eliminated from the model, and the system is maintained at the zero biomass attractor.

Multiplicative noise was also investigated by *Møller et al*. [2009] using a 1-D lake nutrient model. Uniquely, they considered multiplicative state variable noise in addition to a stochastic disturbance. They show that the inclusion of system noise in one of the two state variables can significantly influence the probability of switching attractor basins. *D'Odorico et al*. [2005] investigated multiplicative noise on two attractors derived from a simple deterministic soil moisture-vegetation model. In this case noisy daily rainfall, derived from a Poisson distribution and the rainfall depth from an exponential distribution, was used. They found that the noise-induced stability in the model by eliminating the two basins of attraction and producing a new and intermediate basin of attraction. While these results were interpreted by *Guttal and Jayaprakash* [2007] as simply being due to frequent switching between attractors, this complex interaction between noise and a simple deterministic model has had further support [*D'Odorico et al*., 2007a, 2007b, 2008; *Borgogno et al*., 2009]. Considering that the ecohydrological model investigated within this paper has two sources of multiplicative noise, that is precipitation and potential evapotranspiration, the response to and emergence of both attractors under stochastic forcing may be complex and warrants investigation.

An important differentiating advancement of this paper is the inclusion of a spatial dimension, namely for lateral groundwater flow. A few studies have extended standard 1-D resilience models to 2-D by inclusion of dispersion terms [*von Hardenberg et al*., 2001; *van de Koppel and Rietkerk*, 2004; *van Nes and Scheffer*, 2005] which, while dependent upon the heterogeneity and dispersion rate, were found to result in an expansion to the parameter range producing two attractors [*van de Koppel and Rietkerk*, 2004]. Recently, a

few studies have also applied stochastic forcing to a spatial model [*Dakos et al*., 2010; *Guttal and Jayaprakash*, 2009; *Serizawa et al*., 2009; *Liu et al*., 2008]. Both *Guttal and Jayaprakash* [2009] and *Dakos et al*. [2010] used such a model to investigate measures of spatial variance and correlation as leading indicators for loss of an attractor, i.e., moving from a two attractor configuration to a one attractor configuration. Neither investigated the switching between attractor basins as a result of a disturbance, as was undertaken for 1-D models by *Guttal and Jayaprakash* [2007]. To the author's knowledge, the only quantitative investigations of a stochastic disturbance applied to a spatial resilience model are those of *Serizawa et al*. [2009] and *Liu et al*. [2008]. *Serizawa et al*. [2009] investigated a lake nutrient-phytoplankton model with 2-D diffusion and a 2-D time varying Gaussian disturbance, multiplied to the state variable values and added to the nutrient and phytoplankton rates of change. Of most relevance here, they found that both additive and multiplicative disturbances caused the lake to simply switch to, and persist within, one of the two attractors (i.e., phytoplankton state or a clear water state). The system did not repeatedly switch between the attractor basins nor demonstrate a patch-work of different regions being in different attractor basins. In effect, the system displayed relatively simple attractor dynamics and did not display spatially nested attractor basins of differing scale; a concept known as *panarchy* [*Gunderson and Holling*, 2002]. This finding is in contrast to the lake phytoplankton-zooplankton modeling of *Liu et al*. [2008]. While not directly investigating resilience and multiple attractors, they did demonstrate complex and spatially nested structures can result from the inclusion of sinusoidal forcing and additive stochastic noise. Furthermore, and relating to a similar finding of *D'Odorico et al*. [2005], they found that the inclusion of stochastic noise can increase stability but can also interact with the sinusoidal forcing to produce two distinct frequencies of the periodic phytoplankton concentration linked to the sinusoidal forcing; a process known as *frequency-locking*. Overall, these spatial resilience studies have demonstrated that the inclusion of a spatial dimension can significantly alter the emergence of multiple attractors. With the inclusion of noise, the emergence of spatially heterogeneous or homogeneous attractor structures appears to be dependent upon the specifics of the model and noise, and therefore, it remains an open question at to how the Peterson and Western (submitted manuscript) resilience model will behave under stochastic forcing.

This paper adopts the hypothetical ecohydrological model from the companion paper (Peterson and Western, submitted manuscript). Using the paper's estimate of the state-space location of the attractors and repellor, the emergence of multiple hydrological attractors under daily forcing was investigated by analyzing simulated groundwater hydrographs at multiple locations and parameter values for evidence of a change of attractor basin. Daily forcing was adopted as it was considered to be an adequate compromise between the timescale of relevant hydrological processes, the availability of climate data and the computational requirements. In the following section, the methodology is outlined. Details of the time-integration simulations are presented, followed by the various methods by which the simulation results were analyzed. Section 3 presents the results from analyzing the simulations at various parameter values, locations within the catchments and at various forcing rates. Section 4 presents a discussion of the results and builds upon *Peterson et al*. [2012] to give insights into how multiple hydrological attractors may be detected from field data.

2. Methodology

In assessing stochastic simulations for a change in attractor basins, much of the existing stochastic resilience research has relied upon qualitative inspection of time series results [e.g., *D'Odorico et al*., 2005; *Guttal and Jayaprakash*, 2007]. A quantitative measure proposed by *Scheffer and Carpenter* [2003] is that "*Statistically, the frequency distributions of key variables should be multi-modal if there are alternative attractors*." However, it has been demonstrated that multiple attractors can emerge from stochastic forcing of this hill-slope model without the distribution of depth to water table being bimodal [*Peterson*, 2009; *Peterson et al*., 2009b]. Furthermore, bimodal distributions only emerged if the fraction of time spent within each attractor basin was approximately equal. Therefore, a time series inspection method was adopted for this study. However, to explore the dynamics across space and parameter values, additional graphical analysis was undertaken.

For transparency, the data and Matlab code for the model and continuation analysis are freely available from the supplementary material to Peterson and Western (submitted manuscript). Below, the following aspects of the methodology are detailed: (i) time-integration stochastic simulations and detecting changes in the basin of attraction; and (ii) equilibrium continuation of the model against daily climate forcing. The

latter was undertaken to understand the dynamics observed from the time-integration simulations under stochastic forcing.

2.1. Time-Integration Under Stochastic Forcing

The central question of this paper was whether multiple attractors emerge under stochastic daily forcing. To undertake this investigation, the model, parameter and forcing data where adopted from the companion paper (Peterson and Western, submitted manuscript). From the companion paper, the following results were also obtained from the stochastic forced limit-cycle continuation (SFLCC) analysis: (i) the values of saturated lateral hydraulic conductivity, $k_{s_{max}}$, at which multiple attractors exist under daily forcing; and (ii) the depth to water table of the attractors and repellor, which were used for identifying an attractor basin change in the simulated daily groundwater hydrographs. Initially, all three values of the maximum infiltration parameter, I_o, from Peterson and Western (submitted manuscript) were investigated for this paper. However, like the similarity of the SFLCC results within Peterson and Western (submitted manuscript), the time-integrations results for each value of I_o were very similar. Hence, for this paper an analysis is only presented for a maximum infiltration parameter value of 200 mm d^{-1}.

In undertaking the daily time-integration simulations, the observed daily forcing from Peterson and Western (submitted manuscript) was initially adopted. However, inspection of the simulated groundwater hydrographs showed little evidence of a change in attractor basins. Specifically, the groundwater level persisted within the shallow water table attractor basin because the duration of low rainfall was insufficient to produce a switch to the deep water table attractor basin. To investigate climate series of more extended low rainfall periods, the one hundred climate replicates of daily precipitation and PET and simulations results from *Peterson et al.* [2009b] were analyzed to identify the replicate that produced the largest number of repellor crossings. This replicate was adopted for the daily stochastic simulations within this paper. The climate replicates were derived using The Stochastic Climate Library single site daily climate algorithm [*Srikanthan and Zhou*, 2003; *Srikanthan et al.*, 2007] and the SILO data from 1890 to 2007 inclusively [*Jeffrey et al.*, 2001].

To assess why the selected replicate frequently crossed the repellor, Figure 2 presents empirical cumulative distribution functions of selected statistics from the climate replicates. Statistics from the SILO data and the selected replicate are presented and all data were aggregated to an annual time step to reflect the slow response time of groundwater storage. Figure 2 shows the selected replicate to have a high standard deviation of annual precipitation and PET (relative to the other replicates and the SILO data). This would have caused greater variability in the simulated groundwater level. The mean PET is also shown in Figure 2d to be high and this would cause more rapid drainage to the deep attractor basin. Combined, these two differences most likely explain why the selected replicate frequently crossed the repellor.

Using the selected replicate, time-integration simulations were undertaken at three values of $k_{s_{max}}$ predicted by the SFLCC to have multiple attractors; specifically at 10% (0.41 m d^{-1}), 50% (0.73 m d^{-1}), and 90% (1.05 m d^{-1}) of the two-attractor range (two attractors existed between $k_{s_{max}}$ of 0.33 and 1.13 m d^{-1}). In light of *Peterson et al.* [2012], time-integration simulations were also undertaken at three values of $k_{s_{max}}$ above the two-attractor range; specifically at 150% (1.53 m d^{-1}), 200% (1.93 m d^{-1}), and 400% (3.52 m d^{-1}) of the two-attractor range from the lower fold-point. For each, simulations were conducted with the leaf area index (LAI) positive feedback and without the positive feedback. The initial conditions for each were obtained prior by simulation from an initial fractional saturated thickness of 0.2 and soil moisture fraction of 0.4 using the upscaled climatic forcing to monthly (see Peterson and Western, submitted manuscript for details) for a duration of 200 years. This was undertaken to minimize the duration required for the stochastic simulations to approach an attractor from arbitrary initial conditions, and thus, maximize the period over which the simulations were near independent of the initial conditions. The analysis of the stochastic simulations for the emergence of multiple attractors was undertaken by visually comparing the simulated groundwater hydrographs with the depth to water table of the attractors and repellor.

The surface hydrology from the stochastic simulations was also investigated. This was undertaken by calculating annual flow duration curves from the feedback and nonfeedback model simulations with I_o set to 200 mm d^{-1} and $k_{s_{max}}$ set to 90% (1.05 m d^{-1}) of the two-attractor range. To explore the relationship with depth to water table, each value of daily flow was colored according to the depth to water table at 250 m

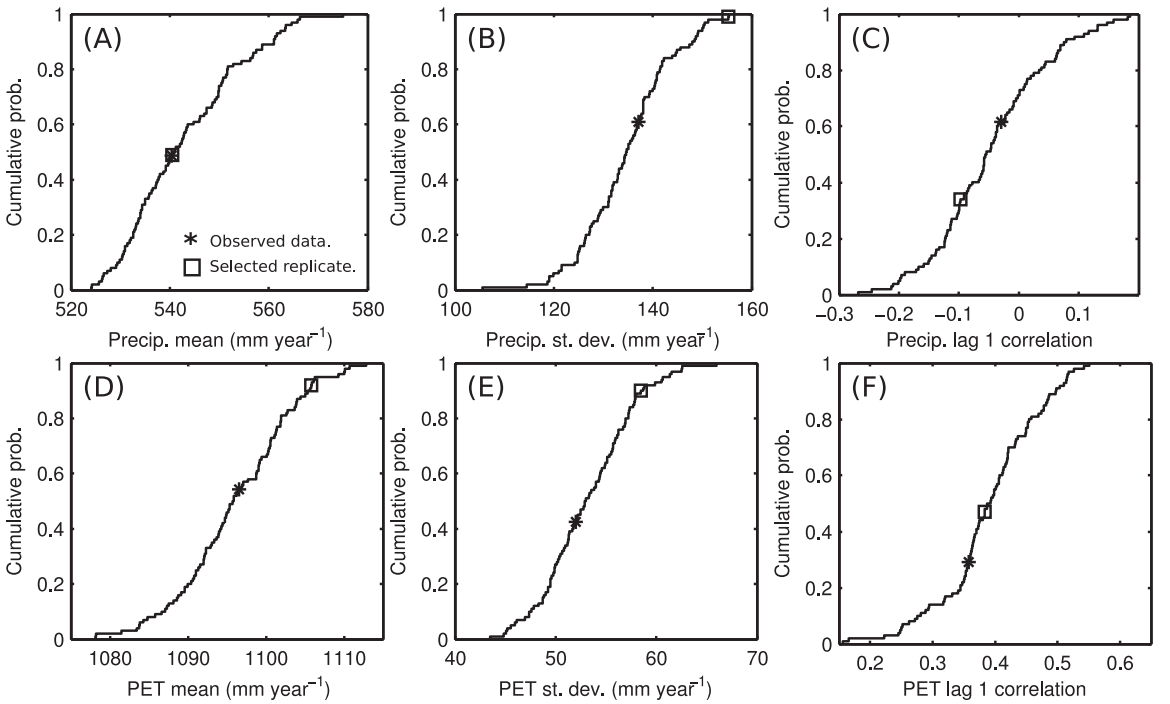

Figure 2. Empirical cumulative distribution functions of climate replicate statistics and point values for the selected replicate and that from the SILO observed data. (a–c) The precipitation annual mean, standard deviation, and lag-1 correlation, respectively. (d–f) The PET annual mean, standard deviation, and lag-1 correlation, respectively. Note that the daily climate data were aggregated to an annual time step prior to calculation of all statistics.

from the catchment outlet. Flow duration curves from the entire simulation were also calculated. In calculating the FDCs, the streamflow was the sum of the daily surface runoff integrated over the hill-slope and the saturated subsurface discharge at the downstream end of the hill-slope.

2.2. Equilibrium Continuation of Climate Forcing

Peterson et al. [2012] demonstrated that for a very simple 1-D groundwater model the switching of attractor basins occurred not by crossing of the repellor but the loss of an attractor during periods of high or low precipitation (see Figure 1 for details). Identification of this mechanism required equilibrium continuation (EC) of the annual precipitation rate and for this investigation a similar analysis was undertaken. To account for this model having both precipitation and PET forcing, the EC was undertaken for a fixed daily PET and the daily precipitation rate was adjusted by the continuation algorithm, along with the model state variable, to identify state-variable values of zero rate of change with time. By repeating the EC at different fixed values of PET, it was possible to develop a two-parameter EC and thereby explore the joint effect of both aspects of the climate forcing. The result is presented as a 3-D plot of PET and precipitation versus depth to water table of the attractors or repellor. To undertake this two-parameter EC, $k_{s_{max}}$ was fixed at 90% of the two-attractor range and the EC for precipitation was repeated at daily PET values of 0.5–14 mm d^{-1} at 0.5 mm d^{-1} increments. To explore the attractors at the other values of $k_{s_{max}}$, the EC was also undertaken at all six values of $k_{s_{max}}$ but the PET was fixed to the mean annual rate of 3.03 mm d^{-1}. The PET was not investigated for a range of $k_{s_{max}}$ values because, relative to precipitation, the variability is low (see Figure 4 of the companion paper).

In analyzing the EC results, the stochastic daily forcing was initially ignored. First, the EC for $k_{s_{max}}$ at 90% of the two-attractor range was investigated to explore the role of PET in the existence of multiple attractors. Next, the results from all six values of $k_{s_{max}}$ were plotted together to give insights into the differing temporal dynamics observed from the stochastic daily simulations. To link the EC results with the stochastic daily simulations, the EC and stochastic simulations results for $k_{s_{max}}$ at 90% of the two-attractor range were overlain. To aid the graphical interpretation, much of the high frequency noise from the simulations was removed. For the precipitation, this was undertaken as follows: (i) daily stochastic precipitation was upscaled to an annual rate; (ii) the annual

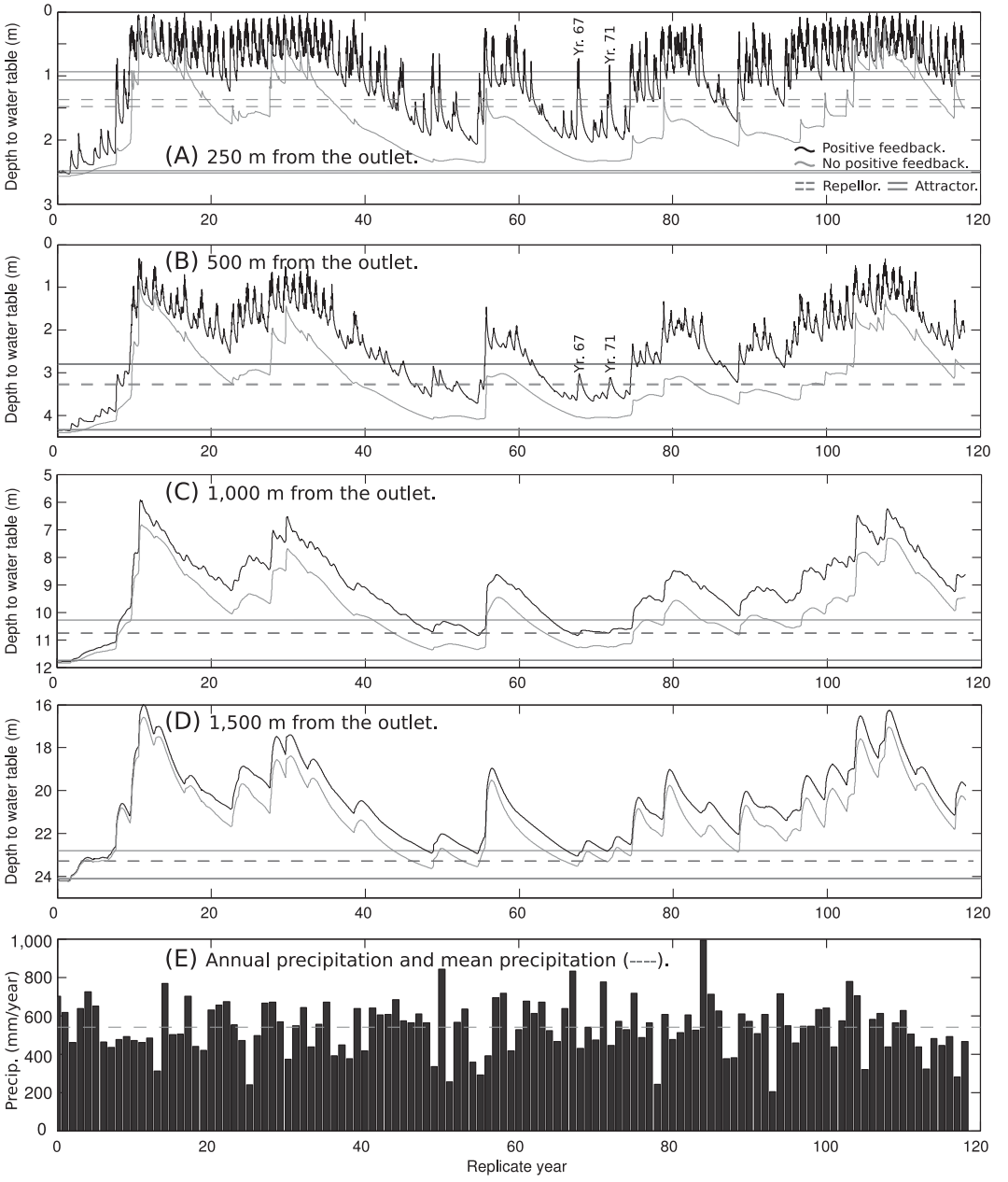

Figure 3. Simulated time series depth to water table at 250, 500, 1000, and 1500 m for $k_{s_{max}}$ at 90% of two-attractor range (1.05 m d^{-1}). Each plot details simulations with and without the positive feedback and the upper and lower extent of the attractors (horizontal solid gray lines) and the repellor (horizontal dashed gray lines).

precipitation was then smoothed using a 2 year moving average window; and (iii) the smoothed precipitation was then interpolated to an end of month value using piecewise Hermite cubic splines. A piecewise Hermite cubic spline was adopted over a standard cubic spline because it produces no overshooting and less oscillation between data points and, hence, in this application produced a more accurate interpolation between the annual time step data points. For the depth to water table at each node of the model, the daily simulation results were smoothed using a 1 year moving average and the depth to water table at the end of each month was extracted. To aid the graphical interpretation of these smoothed results overlain onto the EC results, the rate of change of the depth to water table with time (using a forward finite difference method) was calculate across each month and used to color-code the stochastic results. This graphical analysis was undertaken for simulations with and without the positive feedback.

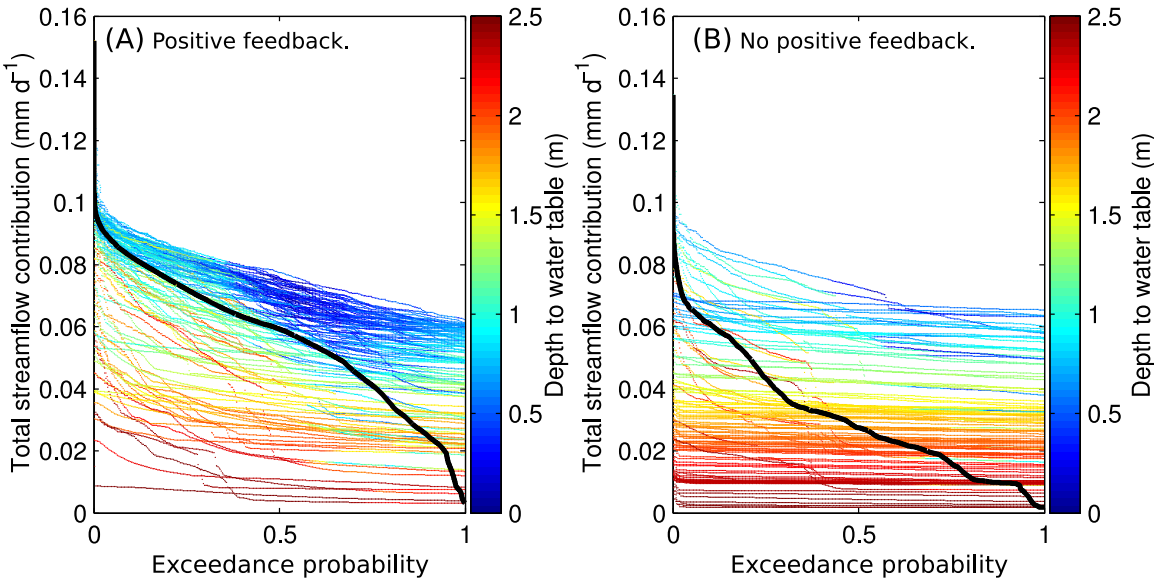

Figure 4. Flow duration curves (FDCs) for (a) the feedback model and (b) the nonfeedback model. The thick black line within each plot is the FDC derived from all 117 years of data. The colored lines denote the annual FDC and the color denotes the depth to water table at 250 m from the catchment outlet.

3. Results

3.1. Evidence for the Emergence of Multiple Attractors

To investigate the emergence of multiple attractors, Figures 3a–3d show the simulated depth to water table hydrographs from the feedback and nonfeedback simulations at four distances from the catchment outlet for $k_{s_{max}}$ of 1.05 m d^{-1}. Each plot also presents the depth to water table of the two attractors and the one repellor. They were obtained from the limit-cycle continuation results of the companion paper and, because the limit-cycle approach accounts for seasonality, each attractor and repellor has an upper and lower bound. Figure 3e shows the annual precipitation and average precipitation of 540 mm y^{-1}.

Within the upper catchment (Figures 3c and 3d), the feedback and nonfeedback simulations were of similar dynamics and water level. Despite the inclusion of the positive feedback and the repeated crossing of the repellor, the feedback model does not show any evidence of multiple attractors emerging. This is most likely to be because the water level did not approach the root-zone. Hence, the positive feedback was not activated at that location and the negative feedback from the aquifer drainage dominated the water level dynamics. The feedback simulations were, however, significantly shallower than the shallow attractor despite there being no evidence that the shallow attractor emerged. This suggests the estimation of attractors under a varying climate is more complex than that presented within the companion paper.

Within the lower catchment (Figures 3a and 3b), the feedback and nonfeedback simulations do have periods of differing dynamics and water level. This is most apparent during the second, fifth, and eighth decade of simulation; during which the water level from the feedback model was approximately 1 m shallower than that from the nonfeedback model. To examine these periods, in the second decade the rainfall declined and the nonfeedback water level subsequently declined but the feedback water level only slightly declined from above the shallow attractor to near to it and then it persisted near the land surface until the forth decade; at which three consecutive years of below average rainfall appears to cause a switch toward the deep attractor. Ignoring the attractors and repellor lines, this persistence at a shallow water level during a low rainfall period suggests the water level was within the shallow attractor basin. Additionally, in the eighth decade the rainfall increased and both the nonfeedback and feedback water level rose but the feedback model water level rose higher to above the shallow attractor line and appears to persist at a shallow depth for a longer duration than that from the nonfeedback model. This suggests the water level switched to the shallow attractor. Conversely, in the fifth decade the rainfall was low and both the nonfeedback and feedback water level declined toward the deep attractor line. Considering that the nonfeedback model only

has a deep water table attractor, caused by the negative feedback from aquifer drainage and evaporation processes, and that the water level from both models converge, it appears that the deep water table attractor did emerge from the feedback-model. Lastly, the shallow attractor lines in the upper catchment appear inconsistent with the simulations. When the water level is simulated as shallow it is often notably shallower than the shallow attractor (Figures 3b–3d)) and only at 250 m from the outlet are the two consistent (Figure 3a). Again, this suggests the estimation of attractors under a varying climate is more complex than that presented within the companion paper. This issue is addressed further within section 3.3.

To explore the dynamics over the whole catchment, Figure 4 shows the annual flow duration curves (FDC) for both the feedback and nonfeedback models. For each model, the FDC derived from the 117 years of simulation is also presented. With regard to the FDC from the whole record, the most striking difference between the models is the considerably higher streamflow from the feedback model at all but the very lowest of exceedance probabilities. For example, the median streamflow contribution from the feedback model was 0.059 mm d^{-1} while that from the nonfeedback model was 0.027 mm d^{-1}, a reduction of 46%. With regard to the annual FDCs, the differences between the models are more pronounced. In particular, a noteworthy difference is in the interannual distributions of flows for a fixed exceedance probability (that is, a vertical slice in Figure 4). In the feedback case (Figure 4a), this distribution is negatively skewed with the majority of annual curves above that from the whole record and associated with shallow water table conditions. For the nonfeedback model, Figure 4b shows the opposite whereby most annual FDCs are below that from the whole record and associated with deep water table conditions.

Overall, including a positive feedback did change the the water table dynamics within the lower catchment (Figures 3a and 3b) and the catchment runoff (Figure 4). There is evidence that both attractors did emerge. However, the evidence is not conclusive and it is ambiguous when the catchment was within each attractor basin. For multiple attractors to unambiguously emerge there would need to be periods in which an extreme rainfall event causes the water table to rise near to the land surface and, upon the climate returning to that prior to extreme event, the water table would need to persists within the shallow attractor until an extreme drought occurs, causing a switch back to the deep water table attractor. That is, for the unambiguous emergence of multiple attractors, the water table would need to be simulated at two distinctly different levels for the same medium term climate forcing. However, considering that climate exerts a continuous disturbance on catchments and that Figure 3a shows an apparent switch to the shallow attractor is not caused by a single extreme climate event, or year, but by a complex interaction of saturated lateral flow and a sequence of moderate climate events, such an unambiguous switching between multiple hydrological attractors appears unlikely.

3.2. Aquifer Conductivity and the Emergence of Multiple Attractors

The prior section presented evidence for the emergence of multiple attractors within the lower catchment. However, the evidence was ambiguous and only one model parameterization was investigated. To further explore the emergence, consider that the deep attractor arises because of the negative feedback from lateral drainage while only the shallow attractor arises because of the positive feedback; that is, from the vegetation LAI-aquifer interactions. Specifically, the shallow attractors exist when there is a water level at which the increased recharge from the positive feedback exceeds the lateral drainage from the negative feedback. Consequently, reducing the strength of the negative feedback should increase the emergence of the shallow attractor, and vice versa, and provide insights into the emergence of multiple attractors. To investigate this, the strength of the negative feedback was varied by changing the saturated lateral hydraulic conductivity, $k_{s_{max}}$. Six values of $k_{s_{max}}$ were investigated. Three were within the $k_{s_{max}}$ range at which two attractors were found to exist (i.e., at 10%, 50%, and 90% of the two-attractor range; two attractors existed between $k_{s_{max}}$ of 0.33 and 1.13 m d^{-1}) and three where above this range where only the deep attractor was estimated to exist (i.e., at 150%, 200% and 400% of the two-attractor range). Figure 5 shows the six simulated depth to water table hydrographs at 250 m from the catchment outlet. For $k_{s_{max}}$ within the two-attractor range, Figures 5a–5c present the depth to water table of the two attractors and the one repellor. They were obtained from the limit-cycle continuation results of the companion paper and, because the limit-cycle approach accounts for seasonality, each attractor and repellor has an upper and lower bound. For $k_{s_{max}}$ above the two-attractor range, Figures 5d and 5e) presents the depth to water table of the deep attractor; which is the only attractor, and hence, no repellor exists.

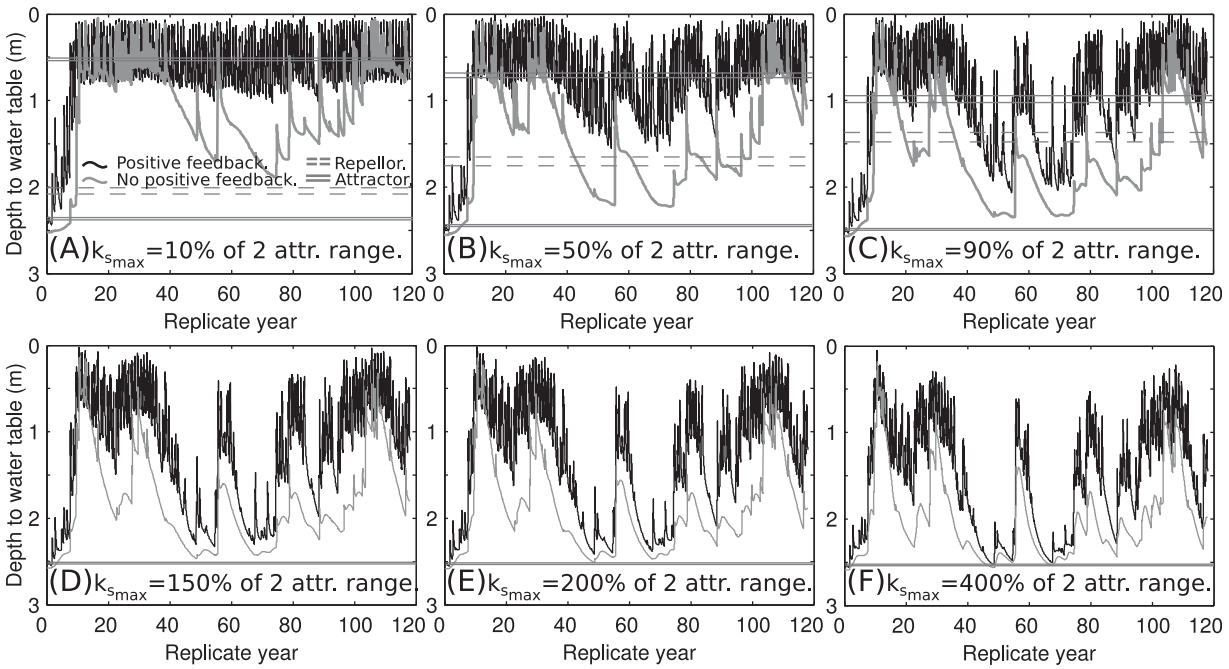

Figure 5. Simulated time series depth to water table at 250 m for (a–c) three $k_{s_{max}}$ values inside the two-attractor range and (d–f) three $k_{s_{max}}$ values above this range. Each plot details simulations with and without the positive feedback and the upper and lower extent of the attractors (horizontal solid gray lines) and the repellor (horizontal dashed gray lines). Year zero denotes the start of the first year of the replicate climate data set. Note, for the plots for three $k_{s_{max}}$ values above the two-attractor range (d–f) only the deep attractor exists.

Considering $k_{s_{max}}$ values within the two-attractor range (i.e., at 10%, 50%, and 90%), Figure 5a shows that, at 10% of this range, the feedback model hydrograph rapidly rises to the shallow attractor and fluctuates around this water level for the remaining simulation. During the forth to tenth decades, the nonfeedback simulation did decline toward the deep attractor but the feedback simulation persisted at a shallow water. This indicates that the shallow attractor could emerge when the negative feedback was weak. However, despite the companion paper estimating two attractors to exist, at no time did the feedback simulation approach the repellor or the deep attractor and, hence, only the shallow attractor emerged.

With the negative feedback increased to $k_{s_{max}}$ at the midpoint of the two-attractor range (i.e., 50%), the feedback model hydrograph rose to slightly above the shallow attractor and remained within the shallow attractor basin (see Figure 5b). During the forth to tenth decades of low rainfall, drainage did bring the hydrograph closer to the repellor. However, despite the companion paper again estimating two attractors to exist, there is no indication of a switching to the deep attractor.

Given that the only evidence for a switching of attractors has arisen for $k_{s_{max}}$ at 90% of the two-attractor range, Figure 5 also presents simulations at 150%, 200%, and 400% of the two-attractor range to investigate if multiple attractors emerge beyond this upper limit. Somewhat surprisingly, the feedback model simulations are very similar to that from $k_{s_{max}}$ at 90% of the two-attractor range and, despite the companion paper indicating the existence of only the deep attractor basin, they appear to show a switching between attractor basins. This is most apparent in Figures 5d and 5e during the second decade of simulation, where the positive feedback simulations persist near to the land surface (relative to the nonfeedback simulations) during years of low rainfall, and during the ninth decade, where a high rainfall period causes the feedback simulation to switch to the shallow attractor but the nonfeedback simulation persists at about 2 m depth to water table. At the highest conductivity, Figure 5f shows the feedback and nonfeedback simulations to converge and the emergence of two attractors is ambiguous.

The above stochastic simulations highlight three subtle resilience concepts. First, detecting the switching between multiple attractors from time series can be difficult and relying on this to identify the existence of multiple attractors can result in misleading conclusions. This is likely to be most pronounced when the disturbance is continuous and a switching of attractors is caused by a sequence of moderate disturbances,

and not a single large disturbance. For the simulations in Figure 5, daily climate forcing exerted such a continuous and moderate forcing and, despite changes in the strength of the negative feedback, evidence for the switching between attractors was somewhat ambiguous. This was despite using a hypothetical model of homogeneous subsurface properties and, assuming some real catchments do have multiple attractors, it suggests why such catchments have not yet been identified.

Second, the switching between attractors does not appear to arise from crossing the repellor (as estimated within the companion paper). To illustrate, Figures 3a and 3b shows that in years 67 and 71 the water level crossed the repellor from the deep attractor and rose to the shallow attractor but very rapidly returned to the deep attractor basin. Figure 3e shows that the water level rose in years 67 and 71 because the precipitation was 291 and 236 mm y^{-1}, respectively, above the average of 540 mm y^{-1}. However, shortly after this the precipitation returned to near the mean for the following 3–5 years but the water level did not persist within the shallow attractor. Considering that the repellor was derived using the long-term average CDF of monthly precipitation (see the companion paper) and hence it informs the water level dynamics only under average climate conditions, the return to near average precipitation and the water level not persisting at a depth of about 0.75 m indicates that, despite the repellor being crossed and the shallow attractor reached, in years 67 and 71 the water level did not switch to the shallow attractor basin. Further confounding the role of the repellor, in the upper catchment Figure 3d shows the water level to be significantly above the shallow attractor prior to the climate events in years 67 and 71 and to have a water level dynamic very similar to that of the nonfeedback model, which has only a deep water level attractor. Obviously the water level dynamics are complicated by the temporal lags from saturated lateral flow, but the repellor does not explain the emergence and switching of hydrological attractors due to climate forcing.

Finally, the existence of multiple attractors, as defined from continuation analysis, can markedly differ from what may emerge under stochastic forcing. Figures 5a–5c shows that for much of the $k_{s_{max}}$ two-attractor range (as estimated by limit cycle continuation within the companion paper), the groundwater level rose rapidly from the deep initial condition and persisted within the shallow attractor basin. The two attractors only appeared to emerge near to the upper limit of the $k_{s_{max}}$ two-attractor range. Additionally, at larger values of $k_{s_{max}}$ for which limit cycle continuation estimated only the deep attractor to exist the water level showed dynamics very similar to that when two attractors did exist. In the following section, this apparent emergence of a shallow attractor and the mechanisms by which a switching of attractors occurs is further investigated.

3.3. Mechanisms Explaining the Emergence of Attractors

Simulations with stochastic forcing produced some unexpected findings. Specifically, a switch of attractor basins did not occur by crossing the repellor and was difficult to detect from the groundwater hydrograph (see Figure 3c). When a switch to the shallow attractor did occur, the water level was predominantly above the shallow attractor (see Figures 3c–3e and 5b). This was most notably so in the upper catchment and as $k_{s_{max}}$ increased. Additionally, at a low value of $k_{s_{max}}$ the companion paper predicted two attractors to exist but only the shallow attractor emerged (see Figures 3a and 3b). Conversely, at a higher value of $k_{s_{max}}$, the companion paper predicted only the deep attractor to exist but stochastic forcing appeared to produce two attractors (see Figures 3d–3f). It is hypothesized that these unexpected findings can be explained by the mechanisms shown in Figure 1, proposed by *Peterson et al*. [2012] and summarized in the introduction.

To explain these mechanisms, *Peterson et al*. [2012] undertook equilibrium continuation for the annual precipitation and a fixed parameter set. By overlaying stochastically simulated groundwater levels, considerable insights were obtained as to how a system may switch attractors. It was shown that if two attractors exist for, say, the mean annual precipitation and the system is within the deep water table attractor, then the water table can only shift to the shallow attractor if the stochastic precipitation is sufficiently high that only the shallow attractor exists. Only if this forcing persists for a sufficient duration will the system shift to the shallow attractor. Another aspect of the switching mechanism is that if, for the mean annual precipitation, only the deep attractor exists then multiple attractors can still emerge during high precipitation periods. To explore if these switching mechanisms apply to the considerably more complex and distributed model investigated here, and explain the unexpected findings of section 3.2, equilibrium continuation was undertaken for precipitation and PET.

In this investigation, quantifying the number of attractors for a given climate forcing has the additional challenge that they depend on both precipitation and PET; not just precipitation as in *Peterson et al*. [2012]. To

overcome this, equilibrium continuation was undertaken for the daily precipitation, with the daily PET fixed; then repeated for a range of mean daily PET values. Figure 6 shows the results for $k_{s_{max}}$ at 90% of the two-attractor range (1.05 m d^{-1}) at 250 and 1000 m from the catchment outlet. At both locations, two attractors clearly emerge when PET is high. Interestingly, as PET declines the extent of the two-attractor precipitation range declines so that at a PET of 2 mm d^{-1} only one attractor exists for the entire range of daily precipitation. This indicates that, in addition to the precipitation switching mechanism of *Peterson et al*. [2012], the loss of an attractor and a subsequent switching of attractors can also occur by a change in PET. That is, for a fixed precipitation and the system within the deep attractor basin, if the PET is high and then significantly declines only the shallow attractor will exist and the system will shift toward it. Conversely, if the system is initially within the shallow attractor and the PET is low, if the PET increases significantly, only the deep attractor will exist and the system will shift toward it. However, considering that PET is typically significantly less variable over time than precipitation, PET was not further investigated.

Figure 7 shows the equilibrium continuation for the daily precipitation repeated for all six values of $k_{s_{max}}$; each with the PET set to the mean rate of 3.03 mm d^{-1}. Most importantly, it shows that at $k_{s_{max}}$ values for which the companion paper found only the deep attractor to exist (specifically, at 150%, 200%, and 400% of the two-attractor range, or 1.53, 1.93, and 3.52 mm d^{-1}, respectively), two attractors clearly exist at higher precipitation rates. For example, for $k_{s_{max}}$ at 150% of two-attractor range, two attractors exist when the precipitation is above 1.25 mm d^{-1} and below 1.3 mm d^{-1}. This is a very narrow two-attractor range but, obviously, precipitation does not occur at a constant rate. Hence it is best to use these equilibrium continuation plots to understand the response to stochastic forcing. That is, if there is an extended period of precipitation above 1.3 mm d^{-1} then the catchment is likely to switch to the shallow attractor and persist there until there is an extended period of below 1.25 mm d^{-1}, upon which the catchment would switch back to the deep attractor. For $k_{s_{max}}$ at 200% of two-attractor range, a comparable wet period is required to switch to the shallow attractor but the switch back to the deep attractor requires a lesser dry period 1.28 mm d^{-1}, making the shallow attractor less likely to emerge. For $k_{s_{max}}$ at 400% of the two-attractor range, the two attractors almost vanish and this explains why the feedback and nonfeedback simulations in Figure 5f are almost identical. In summary, these mechanisms explain why two attractors emerged under stochastic daily forcing at $k_{s_{max}}$ values the companion paper found to have only the deep attractor. The significance of this is that, while only the deep attractor may exist under average precipitation, wet periods may cause the catchment to switch to the shallow attractor and persist within this higher runoff state until an extended period of average, or below average, precipitation occurs.

With regard to the emergence of only the shallow attractor when $k_{s_{max}}$ was at 10% and 50% of the two-attractor range (see Figures 5a and 5b), Figure 7 is less conclusive. For $k_{s_{max}}$ at 10% of the two-attractor range, Figure 7a shows the lower fold-point (that is, the precipitation at which the shallow attractor vanishes) is at about the 10th percentile of the annual precipitation input to the time-integration simulations. Considering that the lower fold-point is also significantly below the median annual precipitation, even a moderate rainfall event could switch the model to the shallow attractor but switching back to the deep attractor would require very low precipitation; and most likely a series of years of very low precipitation because of the slow groundwater drainage rate. Hence, the catchment converges to the shallow attractor over time.

Lastly, when a switch to the shallow attractor did occur, the water level was predominantly above the shallow attractor. This was most notable in the upper catchment (Figures 3b–3d) and as $k_{s_{max}}$ increased (Figures 5b and 5c). Within the upper catchment, Figure 7b shows that, for all six values of $k_{s_{max}}$, the shallow attractor rapidly approaches the land surface as the precipitation increases. So while under average forcing at 1000 m from the outlet the shallow attractor is 10.3 m below the land surface (see Figure 3d), during above average precipitation Figure 7b shows the shallow attractor water level to be significantly shallower. If, during stochastic simulations, such wet periods persist then the water level will approach the shallow attractor depth associated with the higher rainfall. With regard to the changes with $k_{s_{max}}$ within the lower catchment, Figure 7a shows the shallow attractor to only notably move toward the land surface with increased precipitation when $k_{s_{max}}$ is at or above the 90% two-attractor range. By the same mechanism as for the upper catchment, this explains why in Figure 5c the water level, when shallow, is shallower than the shallow attractor for average precipitation and why in Figure 5a the water level, when shallow, oscillates around the shallow attractor.

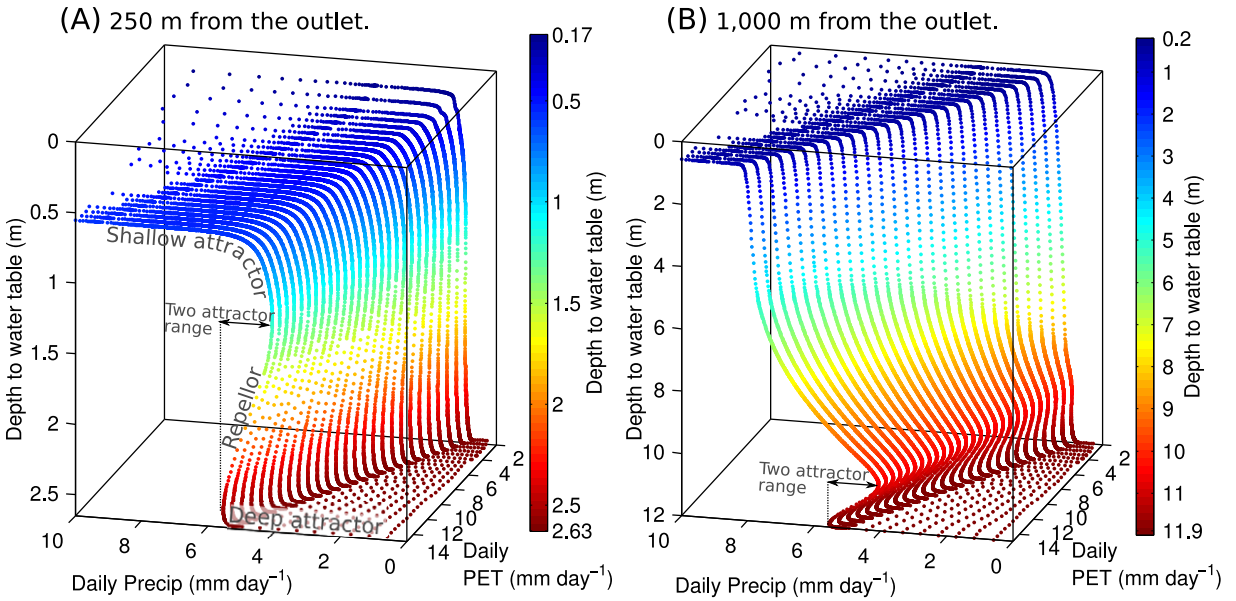

Figure 6. Equilibrium continuation plots at (a) 250 m and (b) 1000 m for daily precipitation repeated at daily PET values of 2–15 mm d^{-1} and with $k_{s_{max}}$ at 90% of two-attractor range (1.05 m d^{-1}).

3.4. Signatures for the Emergence of Multiple Attractors

Detecting a switch of attractor basins from a groundwater hydrograph can be challenging (e.g., see Figure 3a). Unequivocal evidence for the emergence of two attractors would be demonstrated if for different periods with the same climate forcing (and no landuse change), the groundwater level persisted at each of the two attractors. However, the continuous disturbance from climate variability makes such unequivocal evidence unlikely. Alternatively, exploring the interaction of the precipitation attractors from Figure 7 with the stochastic simulations (with and without the positive feedback) may suggest some signatures for the emergence of multiple attractors.

To investigate, Figure 8 shows smoothed simulation results overlain on the equilibrium continuation results at 250 and 1000 m from the catchment outlet. For the nonfeedback simulations, Figures 8c and 8d show

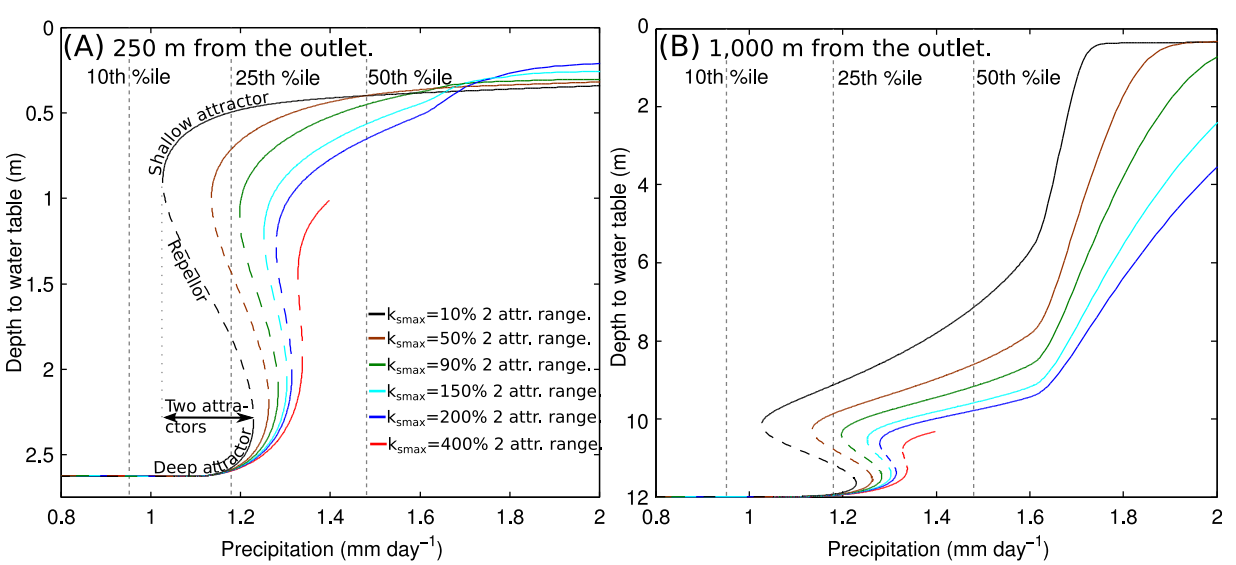

Figure 7. Equilibrium continuation plots at (a) 250 m and (b) 1000 m from the catchment outlet for daily precipitation repeated at all six values of $k_{s_{max}}$. Solid curves denote the attractors, dashed curves denote the repellor between the attractors and the vertical gray dashed lines denote the 10th, 25th, and 50th percentile annual precipitation.

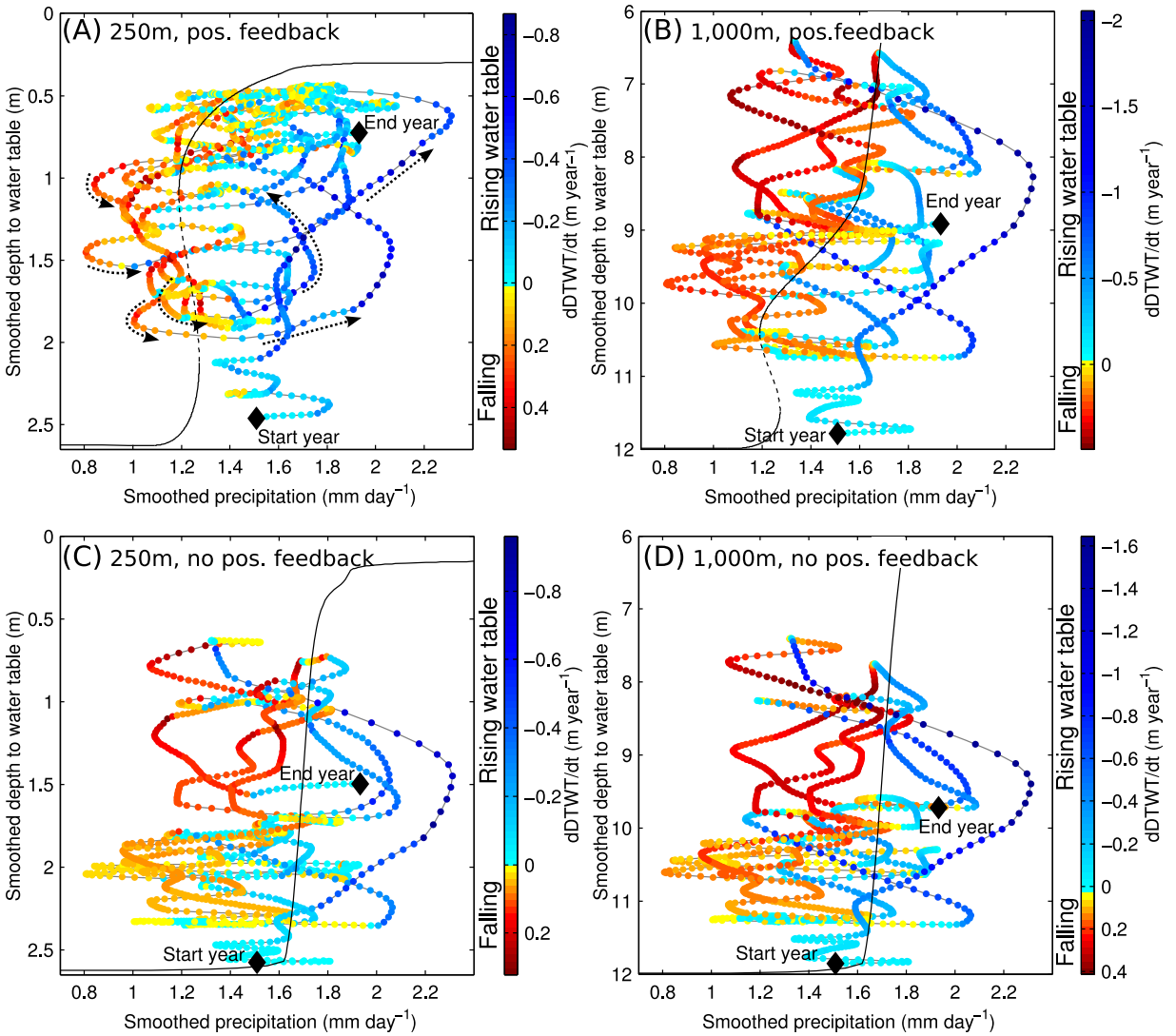

Figure 8. Smoothed stochastic simulation of depth to water table (a and b) with and (c and d) without the positive feedback against the smoothed annual precipitation at (a and c) 250 and (b and d) 1000 m for $k_{s_{max}}$ at 90% of the two-attractor range (1.05 m d^{-1}). The color of each dot denotes the annual rate of change in the depth to water table, dots are at monthly time steps, the continuous black line denotes the attractors and the dashed black line in Figures 8a and 8b denotes the repellor. To illustrate the direction of time, in Figure 8a, selected periods of the simulation are annotated by dashed arrows.

the response to precipitation in the upper and lower catchment to be very similar. At both locations the water table is often deep (relative to the feedback simulations) and during years of high precipitation the water table rises rapidly (see aqua and blue dots on right side of each figure) and then declines back to the deep state following the period of high rainfall; hence, reaffirming the nonexistence of the shallow attractor. Also, the groundwater level does not appear to converge to the deep attractor. Despite the precipitation being the 2 year moving average, the continuous forcing from precipitation and PET never persist at a constant rate for a sufficient duration for the water level to converge to the deep attractor. The time to convergence is clearly a function of the soil and aquifer hydraulic properties and the catchment size, but it illustrates that even without a positive feedback the influence of a single attractor is subtle.

With a positive feedback, Figures 8a and 8b show the response to precipitation in the upper and lower catchment to be dissimilar. The upper catchment feedback simulation is similar to the nonfeedback simulation (see Figures 8b and 8d) in that the water table does not appear to persist at the shallow attractor following a period of high precipitation. Conversely, in the lower catchment Figure 8a shows the water table to clearly persist within the shallow attractor. This is illustrated by the large number of months (circles are at

monthly time steps) where the water table is shallow and its smoothened rate of change is approximately zero (denoted by yellow and aqua dots). When a low precipitation period occurs the water level declines toward the deep attractor (see lines of red dots on left of plot) but does not reach the deep attractor or persist within the deep attractor basin; as illustrated by there being few months of zero rate of change. While this is partially a function of the 1 year moving-average smoothing of the water level and aquifer drainage being a slower processes than recharge, there is a wider distribution of zero gradient points with depth when a positive feedback exists (see Figures 8a and 8c). Additionally, the switching from a deep to shallow water level, and vice versa, occurs over a wider range of precipitation. Specifically, the hysteresis loop elongates in that, when the positive feedback exists, the water table declines toward the deep attractor during periods of lower precipitation (compare the lines of red dots on left of Figures 8a and 8c). This indicates that a change of water level is occurring by exceedance of a fold-point. However, a change of attractor basins requires not only exceedance of a fold point but a disturbance of sufficient duration so that upon returning to average forcing conditions the system is within a different attractor basin (see Figures 1h and 1j). If the duration is insufficient then the system will return toward the original attractor. Considering that drainage is a slower process than recharge, this mechanism is likely to also explain the numerous counter-clockwise loops in Figure 8a that do not result in a switch to the deep attractor; that is, a wet period event occurs before drainage has had time to cause a change of attractor basins.

Overall, within the lower catchment, the distribution of zero gradient points over a range of water table depths and the wider range of precipitation over which a change of water level occurs provides some signatures indicative of multiple attractors emerging. The mechanism for a change of attractors, while less conclusive than that from the 1-D model of *Peterson et al*. [2009a], is consistent with that proposed to explain the time-integration results in Figure 5 and as proposed within Figure 1. However, using these signatures to reliably identify catchments having switched attractor basins would be challenging. This is because, even without a positive feedback, continuous climate forcing made identifying the single attractor difficult (see Figures 8c. Furthermore, observed groundwater hydrographs may be of insufficient record length relative to the frequency of switching to detect elongated counter-clockwise loops proposed to be indicative of switching between multiple attractor basins.

4. Discussion and Conclusions

The companion paper (Peterson and Western, submitted manuscript) showed that two attractors can exist under stochastic daily forcing within a hill-slope surface-groundwater model having a positive feedback arising from an empirical relationship between LAI and the water table. This paper explored whether stochastic daily forcing can cause the simulated catchment to switch between both attractors; that is, whether the attractors that exist can also emerge under stochastic daily forcing. At a range of saturated lateral conductivity values both attractors were found to emerge under stochastic daily forcing. However, the emergence of attractors was found to be subtle and significantly more complex than those attractors that existed and the behavior expected from standard resilience concepts [*Walker et al*., 2004; *Gunderson and Holling*, 2002].

This paper has shown that the existence of a positive feedback can have a clear impact on the catchment runoff and the groundwater level. However, identifying the switching between attractor basins from groundwater hydrographs is subtle and challenging. This is primarily due to climate exerting a continuous disturbance and, when a change of attractor basins does occur, it is a complex function of historic climate and not a single extreme event. Additionally, the water table depth of the attractor basin to which the catchment switches continuously changes with the climate; hence making convergence to the attractor unlikely. Combined with the temporal lags from lateral groundwater flow, it is, in retrospect, not surprising that identifying the emergence of multiple hydrological attractors is challenging. If some real catchments do have multiple attractors and these catchments have switched between them, we suspect that it is because of these challenges that they have not yet been identified.

With regard to the emergence of attractors, the first complex aspect was that, while two attractors may exist, over time a stochastically forced system may converge to only one of the attractors. This was found to occur at low values of lateral saturated hydraulic conductivity, $k_{s_{max}}$. For these cases, the stochastic forced limit-cycle continuation (SFLCC) predicted two water table attractors but under stochastic forcing the shallow attractor became asymptotically stable; that is, over time the system converged too and remained

within the shallow attractor. Continuation analysis against precipitation showed that this behavior was likely to be due to precipitation predominately being above the lower precipitation fold-point. That is, the precipitation was never low enough, for a long enough period, to displace the system to a state having only the deep attractor. The emergence of asymptotic stability of the shallow attractor is probably due to the difference in response times between the rapid response from recharge and the very slow response from lateral drainage. At higher values of $k_{s_{max}}$, lateral drainage was sufficient relative to the duration of low rainfall periods to allow drainage to the deep attractor. With regard to identifying actual catchments with multiple attractors, analysis of historic observation data would most likely be unable to distinguish between a catchment having only the shallow attractor and a catchment having this asymptotically stable shallow attractor.

The second complex aspect of the emergence of attractors was that a temporary shallow attractor can emerge during periods of high precipitation. This was found to occur at high values of lateral saturated hydraulic conductivity, $k_{s_{max}}$, that SFLCC predicted to have only the deep attractor. By quantifying the number of attractors against daily precipitation, the temporary shallow attractor was found to emerge because only the shallow attractor existed during periods of very high precipitation. If this wet period was of sufficient duration relative to the lateral drainage, then the system shifted to the shallow attractor. Once precipitation returned to the mean, only the deep attractor existed and the system drained toward it. With regard to identifying actual catchments with multiple attractors, analysis of observation data may reveal a switching between two attractors but it is unlikely that analysis could discriminate between a shallow attractor that can emerge during average climate periods and one that emerges only during wet periods and, hence, is more transient. Furthermore, and counter to the findings of the companion paper, the existence of a temporary shallow attractor over a wide range of $k_{s_{max}}$ values indicates that more catchments may display some form of multiple hydrological attractors than previously considered.

To summarize the above findings: (i) an attractor may exist but never emerge; (ii) both attractors may exist and both may emerge; and (iii) only one attractor may exist at the mean forcing but a second temporary attractor may emerge only during certain periods of stochastic forcing. Overall, these findings illustrate a strong interaction between the existence of an attractor and the stochastic forcing. While the continuation analysis for a model parameter, for example $k_{s_{max}}$ within the companion paper, is a useful technique for identifying if an attractor could possibly emerge under average forcing, it could not have identified these mechanisms. The existence of a second attractor during periods of extreme stochastic forcing can be identified by continuation of the precipitation (see Figure 7) but to identify if the attractor is temporary requires the climate scaling continuation analysis of the companion paper to assess if two attractors exist under average forcing. Additionally, continuation analysis of the precipitation cannot distinguish between an attractor basin that forcing causes repeated switching into and out of, and an attractor basin that is asymptoticly stable; that is, the system converges to it and forcing cannot cause a switch back to the other attractor. Identifying an attractor that cannot emerge under current climate forcing may appear irrelevant to catchment management, however, knowledge of alternative attractors to those that have emerged could prove useful. For example, as a result of land use change or climate change the resilience of the emergent attractor may decline (that is, a smaller climate event may be required for the emergent attractor to disappear), making a change of attractor basins more likely. Alternatively, the current attractor the system is within may be undesirable from a management perspective and intervention, such as groundwater pumping, could be applied to cause a switch to a more desirable attractor basin. A final, and more subtle, weakness of continuation analysis of the forcing rate is that the water table depth of attractors may be unreliable (for example see the shallow attractor estimate for $k_{s_{max}}$ of 1.05 m d^{-1} within Figures 7a and 4c within Peterson and Western (submitted manuscript)) and hence the approach should be primarily used to quantify the number attractors. Overall, despite the shortcomings of equilibrium continuation of the precipitation rate, it does appear to be the most viable method for identifying the existence of multiple attractors. Furthermore, the technique is numerically simpler than limit-cycle continuation analysis and this would allow application to more complex models.

Combining equilibrium continuation with observed groundwater data appears to be a promising approach for identifying an historic switching between multiple attractor basins. Figure 8a demonstrated that an elongation of a counter-clockwise hysteresis loop to a wider range of precipitation rates within the lower catchment may be one indicator of attractor switching. Other data analysis methods have been proposed that use moving window statistics of the observation data as a leading indicator of a change of attractor basins [*Guttal and Jayaprakash*, 2009; *Dakos et al*., 2010; *Biggs et al*., 2009]. Importantly, each of these statistical

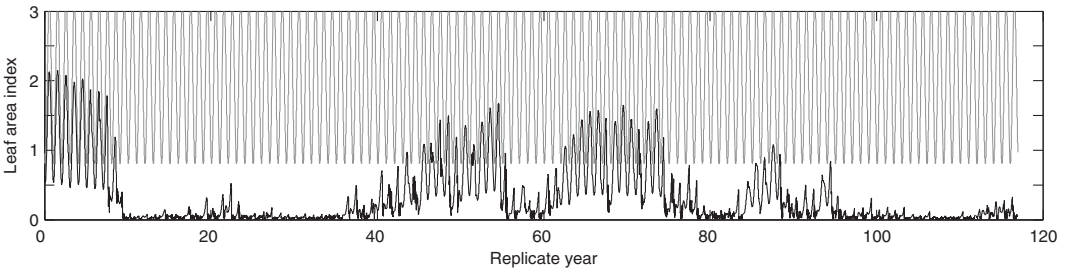

Figure 9. Leaf area index over time at 250 m for $k_{s_{max}}$ at 90% of two-attractor range (1.05 m d^{-1}). The black line denotes the simulation with the positive feedback and the gray line the simulation without the positive feedback.

methods was developed for a change of attractors occurring by exceedance of a fold-point, rather than by crossing the repellor. Considering that this paper and *Peterson et al*. [2012] showed that a catchment changes attractors by exceedance of a fold-point, these statistical measures may be applicable to catchment hydrology. However, whatever method is most appropriate, any foreseeable method for identifying an historic switch between multiple attractor basins will most likely be complicated by nonstationary catchment processes. For a catchment in which, say, native vegetation was progressively cleared over the preceding decades, the water table would likely rise. Distinguishing this rise from a rise resulting from a wet period causing a switch to a shallow attractor would be challenging. Furthermore, the clearing of the native vegetation would most likely cause a change in the number of attractors [*Anderies*, 2005] and, if two attractors did continue to exist after the clearing, then the precipitation range over which two attractors exist would most likely also change. Considering that most gauged catchments have undergone, or are undergoing, anthropogenic land use change it is going to be challenging to distinguish a switch of hydrological attractors from a hydrological change resulting from nonstationary processes.

Shifting away from resilience concepts, at each of the two attractors the LAI differed by at least one order of magnitude. To illustrate, Figure 9 shows the LAI from the feedback and nonfeedback models for $k_{s_{max}}$ at 90% of the two-attractor range (1.05 m d^{-1}) at 250 m from the catchment outlet. For the nonfeedback model, the LAI varies seasonally from 0.81 to 3.2 but does not change from year to year. For the feedback model the LAI changes significantly from year to year and it responds very quickly to changes in the depth to water table (Figure 3a), declining toward zero when the water table is near the land surface. This raises two important questions. First, is the LAI from the feedback model realistic and, if not, what are the implications for the findings? Field studies of vadose zone-water table interaction have shown a very large reduction in LAI for shallow saline water tables. *Zhang et al*. [1999] undertook a two site lysimeter study of irrigated lucerne with a 1 m deep water table and found that with a change from fresh (0.1 dS m^{-1}) to saline (16 dS m^{-1}) water table, the LAI declined by 41% and transpiration declined by 36%. For trees, *Benyon et al*. [1999] found that after 7 years growth at sites of moderately saline shallow groundwater the leaf area of *E. camaldulensis* and *E. occidentalis* decreased by 50% and 61%, respectively, compared to fresh groundwater sites. The simulated reduction in LAI is, however, at least 90%. If the model was parameterized to simulate a lesser reduction in LAI, then when the water table is shallow the transpiration would increase and the recharge would decline from that simulated above. As to whether the shallow attractor would still exist under *average* climate forcing, this is dependent upon the aquifer lateral flow. However, if the shallow attractor no longer existed, a temporary attractor is likely to exist during wet periods. In summary, the simulation of a more plausible reduction in LAI may change the parameter range over which multiple attractors exist and emerge but is unlikely to eliminate them for all catchment configurations and invalidate the findings from this hypothetical study.

The second question arising from the large reduction in LAI, is whether the two attractors emerge only because of the obvious fact that a change in land cover produces different recharge rates that result in different water table elevations? The causal pathway for this question, and many land cover-groundwater investigations, is of a vegetation change (which is almost always assumed anthropogenic) driving the change in the water table elevation. However, the multiple attractors emerge because of the reverse pathway. That is, a change in water table elevation drives a change in land cover via a change in the fraction of the root zone within the saline water table which causes a proportional change in the LAI. If a water table disturbance is sufficient to produce a change in the LAI then a positive feedback can be initiated causing an amplification of the disturbance, resulting in a significant change in the LAI and new equilibrium water table

elevation. If the traditional pathway of land cover change driving changes in the water table were operating then such complex disturbance-response behavior would not exist, only one attractor could exist and the system would have infinite resilience to disturbances.

Looking more broadly at the implications for hydrology, nonlinear uncertainty analysis has received considerable attention over the preceding decade. Considering the scenario of calibrating a conceptual rainfall-runoff model that has no positive feedback (and hence only one attractor) to a catchment that has switched between two attractors, then there are likely to be step changes in the residuals between the modeled and observed flow associated with attractor changes. If only the parameter uncertainty was considered then the uncertainty in each parameter could be either under or over estimated, depending on the exact approach and error model assumptions made. If the uncertainty analysis was undertaken for the combination of input and output data and the parameters, then the uncertainty would likely be incorrectly partitioned between the parameters and the data. In all methods there would be a substantial structural uncertainty that is unlikely to be well represented. Obviously such structure error could be caused by many factors but it could be one indicator of multiple attractors having emerged. Alternatively, if such a model was calibrated to a catchment in which a switch of attractors had not yet been observed, but could occur, then even if reliable error models were derived for all data and parameters and the total prediction error was rigorously defined, then a future switching of attractors would present an emergent uncertainty unaccounted for in the uncertainty analysis. While these scenarios may be somewhat alarmist, they do highlight that the structural uncertainty arising from an unforeseen change of attractors represents a systemic change in the catchment dynamics that would most likely be quite persistent. If, however, such structural errors could be quantified then it may offer a means for identifying multiple attractors within streamflow records. *Renard et al*. [2011] showed that, provided the data error models are reliable, the structural uncertainty can be quantified as a residual from the total errors. While such structural uncertainty may result from other deficiencies of the model, not just the omission of a positive feedback, such residual analysis of models with and without feedbacks leading to multiple states could provide another means for identifying multiple attractors in the field.

This paper aimed to investigate if multiple hydrological attractors can emerge under stochastic forcing. By investigating a single climate replicate in detail, numerous insights were obtained that are felt to have relevance to hydrology and the wider field of ecosystem resilience. Using numerous replicates, further research could quantify the probability of switching attractor basins [e.g., *Peterson et al*., 2009b; *Møller et al*., 2009]. However, all such findings would still be based upon a model that, like any model, has numerous assumptions and simplifications [see *Peterson et al*., 2009a]; which, if overcome, may eliminate the existence of multiple attractors or make them exceedingly rare and difficult to detect in the field. This paper has provided some insights into what hydrologists should be looking for when trying to detect an attractor switch. Future research will attempt to use this to identify groundwater hydrograph properties that indicate a switching of attractors. Hopefully, this will reduce the reliance upon deterministic models and provide a basis for identifying real catchments actually having multiple attractors.

Acknowledgments
The authors are grateful for the support received from the Australian Research Council (grant LP0991280), the Department of Sustainability and Environment, Victoria, Australia; the Department of Primary Industries, Victoria, Australia; and the Bureau of Meteorology, Australia. The authors also thank Murugesu Sivapalan, Stan Schymanski and a third anonymous reviewer for their valuable comments and suggestions.

References

Anderies, J. M. (2005), Minimal models and agroecological policy at the regional scale: An application to salinity problems in southeastern Australia, *Reg. Environ. Change*, *5*(1), 1–17, doi:10.1007/s10113-004-0081-z.

Beisner, B. E., D. T. Haydon, and K. Cuddington (2003), Alternative stable states in ecology, *Frontiers Ecol. Environ.*, *1*(7), 376, doi:10.2307/3868190.

Benyon, R. G., N. E. Marcar, D. F. Crawford, and A. T. Nicholson (1999), Growth and water use of Eucalyptus camaldulensis and E-occidentalis on a saline discharge site near Wellington, NSW, Australia, *Agric. Water Manage.*, *39*(2–3), 229–244.

Biggs, R., S. R. Carpenter, and W. A. Brock (2009), Turning back from the brink: Detecting an impending regime shift in time to avert it, *Proc. Natl. Acad. Sci. U. S. A.*, *106*(3), 826–831, doi:10.1073/pnas.0811729106.

Borgogno, F., P. D'Odorico, F. Laio, and L. Ridolfi (2009), Mathematical models of vegetation pattern formation in ecohydrology, *Rev. Geophys.*, *47*, RG1005, doi:10.1029/2007RG000256.

Carpenter, S. R., and R. C. Lathrop (2008), Probabilistic estimate of a threshold for eutrophication, *Ecosystems*, *11*(4), 601–613.

Dakos, V., E. H. van Nes, R. Donangelo, H. Fort, and M. Scheffer (2010), Spatial correlation as leading indicator of catastrophic shifts, *Theor. Ecol.*, *3*(3), 163–174, doi:10.1007/s12080-009-0060-6.

D'Odorico, P., and A. Porporato (2004), Preferential states in soil moisture and climate dynamics, *Proc. Natl. Acad. Sci. U. S. A.*, *101*(24), 8848–8851.

D'Odorico, P., F. Laio, and L. Ridolfi (2005), Noise-induced stability in dryland plant ecosystems, *Proc. Natl. Acad. Sci. U. S. A.*, *102*(31), 10,819–10,822, doi:10.1073/pnas.0502884102.

D'Odorico, P., K. Caylor, G. S. Okin, and T. M. Scanlon (2007a), On soil moisture-vegetation feedbacks and their possible effects on the dynamics of dryland ecosystems, *J. Geophys. Res.*, *112*, G04010, doi:10.1029/2006JG000379.
D'Odorico, P., F. Laio, A. Porporato, L. Ridolfi, and N. Barbier (2007b), Noise-induced vegetation patterns in fire-prone savannas, *J. Geophys. Res.*, *112*, G02021, doi:10.1029/2006JG000261.
D'Odorico, P., F. Laio, L. Ridolfi, and M. Lerdau (2008), Biodiversity enhancement induced by environmental noise, *J. Theor. Biol.*, *255*(3), 332–337.
D'Odorico, P., V. Engel, J. Carr, S. Oberbauer, M. Ross, and J. Sah (2011), Tree-grass coexistence in the everglades freshwater system, *Ecosystems*, *14*(2), 298–310, doi:10.1007/s10021-011-9412-3.
Gunderson, L. H., and C. S. Holling (Eds.) (2002), Panarchy: Understanding Transformations in Human and Natural Systems, 507 pp., Island Press, Washington, D. C.
Guttal, V., and C. Jayaprakash (2007), Impact of noise on bistable ecological systems, *Ecol. Modell.*, *201*(3–4), 420–428, doi:10.1016/j.ecolmodel.2006.10.005.
Guttal, V., and C. Jayaprakash (2009), Spatial variance and spatial skewness: Leading indicators of regime shifts in spatial ecological systems, *Theor. Ecol.*, *2*(1), 3–12, doi:10.1007/s12080-008-0033-1.
Heffernan, J. (2008), Wetlands as an alternative stable state in desert streams, *Ecology*, *89*(5), 1261–1271, doi:10.1890/07-0915.1.
Hilt, S., J. Kohler, H. P. Kozerski, E. H. van Nes, and M. Scheffer (2011), Abrupt regime shifts in space and time along rivers and connected lake systems, *Oikos*, *120*(5), 766–775, doi:10.1111/j.1600-0706.2010.18553.x.
Holling, C. S. (1973), Resilience and stability of ecological systems, *Annu. Rev. Ecol. Syst.*, *4*, 1–23, doi:10.1146/annurev.es.04.110173.000245.
Jeffrey, S. J., J. O. Carter, K. B. Moodie, and A. R. Beswick (2001), Using spatial interpolation to construct a comprehensive archive of Australian climate data, *Environ. Modell. Software*, *16*(4), 309–330, doi:10.1016/S1364-8152(01)00008-1.
Liu, Q., Z. Jin, and B. Li (2008), Resonance and frequency-locking phenomena in spatially extended phytoplankton-zooplankton system with additive noise and periodic forces, *J. Stat. Mech.*, *5*, P05011, doi:10.1088/1742-5468/2008/05/P05011.
Ludwig, D., B. H. Walker, and C. S. Holling (1997), Sustainability, stability, and resilience, *Conserv. Ecol.*, *1*(1), 7. [Available at: http://www.consecol.org/vol1/iss1/art7/.]
May, R. M. (1977), Thresholds and breakpoints in ecosystems with a multiplicity of stable states, *Nature*, *269*(5628), 471–477.
Møller, J. K., J. Carstensen, H. Madsen, and T. Andersen (2009), Dynamic two state stochastic models for ecological regime shifts, *Environmetrics*, *20*(8), 912–927, doi:10.1002/env.962.
Peterson, T. J. (2009), *Multiple hydrological steady states and resilience*, PhD thesis, Dep. Civ. Environ. Eng., Univ. of Melbourne, Parkville. [Available at: http://repository.unimelb.edu.au/10187/8540.]
Peterson, T. J., R. M. Argent, A. W. Western, and F. H. S. Chiew (2009a), Multiple stable states in hydrological models: An ecohydrological investigation, *Water Resour. Res.*, *40*, W03406, doi:10.1029/2008WR006886.
Peterson, T. J., and A. W. Western (2014), Multiple hydrological attractors under stochastic daily forcing: 1. Can multiple attractors exist?, *Water Resour. Res.*, *50*, doi:10.1002/2012WR013003.
Peterson, T. J., A. W. Western, and R. M. Argent (2009b), Multiple hydrological stable states and the probability of climate variability causing a threshold crossing, in 18th IMACS World Congress and MODSIM09 International Congress on Modelling and Simulation, edited by R. Anderssen, R. Braddock, and L. Newham, pp. 3109–3115, Model. and Simul. Soc. of Aust. and N. Z. and Int. Assoc. for Math. and Comput. in Simul., Cairns, Queensland, Australia.
Peterson, T. J., A. W. Western, and R. M. Argent (2012), Analytical methods for ecosystem resilience: A hydrological investigation, *Water Resour. Res.*, *48*, W10531, doi:10.1029/2012WR012150.
Renard, B., D. Kavetski, E. Leblois, M. Thyer, G. Kuczera, and S. W. Franks (2011), Toward a reliable decomposition of predictive uncertainty in hydrological modeling: Characterizing rainfall errors using conditional simulation, *Water Resour. Res.*, *47*, W11516, doi:10.1029/2011WR010643.
Rennermalm, A. K., J. M. Nordbotten, and E. F. Wood (2010), Hydrologic variability and its influence on long-term peat dynamics, *Water Resour. Res.*, *46*, W12546, doi:10.1029/2009WR008242.
Runyan, C., and P. D'Odorico (2010), Ecohydrological feedbacks between salt accumulation and vegetation dynamics: Role of vegetation-groundwater interactions, *Water Resour. Res.*, *46*, W11561, doi:10.1029/2010WR009464.
Scheffer, M., and S. R. Carpenter (2003), Catastrophic regime shifts in ecosystems: Linking theory to observation, *Trends Ecol. Evol.*, *18*(12), 648–656.
Scheffer, M., S. R. Carpenter, J. A. Foley, C. Folke, and B. H. Walker (2001), Catastrophic shifts in ecosystems, *Nature*, *413*(6856), 591–596.
Serizawa, H., T. Amemiya, and K. Itoh (2009), Noise-triggered regime shifts in a simple aquatic model, *Ecol. Complexity*, *6*(3), 375–382, doi:10.1016/j.ecocom.2009.03.002.
Srikanthan, R., and S. Zhou (2003), Stochastic generation of climate data, *Tech. Rep. 03/12*, Coop. Res. Cent. For Catch. Hydrol. Australia.
Srikanthan, R., F. H. S. Chiew, and A. Frost (2007), Stochastic climate library: User guide, technical report, CRC for Catch. Hydrol., Melbourne, Australia.
van de Koppel, J., and M. Rietkerk (2004), Spatial interactions and resilience in arid ecosystems, *Am. Nat.*, *163*(1), 113–121.
van Nes, E. H., and M. Scheffer (2005), Implications of spatial heterogeneity for catastrophic regime shifts in ecosystems, *Ecology*, *86*(7), 1797–1807.
von Hardenberg, J., E. Meron, M. Shachak, and Y. Zarmi (2001), Diversity of vegetation patterns and desertification, *Phys. Rev. Lett.*, *87*(19), 198,101–198,104.
Walker, B. H., D. Ludwig, C. S. Holling, and R. M. Peterman (1981), Stability of semi-arid savanna grazing systems, *J. Ecol.*, *69*(2), 473–498.
Walker, B. H., C. S. Holling, S. R. Carpenter, and A. Kinzig (2004), Resilience, adaptability and transformability in social-ecological systems, *Ecol. Soc.*, *9*(2), 5. [Available at http://www.ecologyandsociety.org/vol9/iss2/art5/.]
Zhang, L., W. R. Dawes, P. G. Slavich, W. S. Meyer, P. J. Thorburn, D. J. Smith, and G. R. Walker (1999), Growth and ground water uptake responses of lucerne to changes in groundwater levels and salinity: Lysimeter, isotope and modelling studies, *Agric. Water Manage.*, *39*(2–3), 265–282.